Novel π-Conjugated Systems Based on Pyrimidine *N*-Oxide

Kseniya N. Sedenkova,[a,b] Julia V. Kolodyazhnaya,[a] Dmitry A. Vasilenko,[a] Yulia A. Gracheva,[a] Elena V. Kharitonoshvili,[a] Yuri K. Grishin,[a] Alexey A. Chistov,[c,d] Victor B. Rybakov,[a] Tina Holt,[e] Andrei G. Kutateladze,[e] Tamara S. Kuznetsova,[a] Elena R. Milaeva[a,b] and Elena B. Averina* [a,b]

[a] *Department of Chemistry, Lomonosov Moscow State University, Leninskie Gory, 1–3, Moscow 119991, Russia. E-mail: elaver@med.chem.msu.ru*

[b] *IPhaC RAS, Severnyi Proezd, 1, Chernogolovka, Moscow Region, 142432, Russia.*

[c] *Shemyakin-Ovchinnikov Institute of Bioorganic Chemistry, Miklukho-Maklaya 16/10, Moscow 117997, Russia.*

[d] *Orekhovich Research Institute of Biomedical Chemistry, Pogodinskaya 10, Moscow 119121, Russia.*

[e] *Department of Chemistry and Biochemistry, University of Denver, Denver, Colorado, 80208, USA.*

Abstract. Pyrimidine *N*-oxide moiety for the first time was used as a heterocyclic core for the construction of π-conjugated molecules with fluorescent properties. For the synthesis of the title compounds a simple two-step protocol starting from readily available 4-fluoro-2-methylpyrimidine *N*-oxides was elaborated. A series of 17 novel pyrimidine *N*-oxide derivatives containing various functional substituents and π-conjugated systems of different length were obtained. The title compounds revealed fluorescent properties in visible region, possessing emission maximum up to 575 nm. Deoxygenation of the *N*-oxide group led to the loss of visible fluorescence. The chemosensor properties towards TFA and a number of metal cations were demonstrated for **3a**, the first representative of the title series. Cytotoxic activity against breast adenocarcinoma cell line was found for three pyrimidine *N*-oxide derivatives **3b,i,n**. Pyrimidine *N*-oxide **3a** was shown to possess excellent biocompatibility and capability to enter cells, that makes it a promising structure for development of bioimaging fluorescent probes.

Keywords: Pyrimidines, π-Conjugated systems, Knoevenagel condensation, Fluorescence, Metal cations, Anticancer activity

1. Introduction

Pyrimidine is an ubiquitous heterocyclic scaffold, particularly important in living organisms as a core of pyrimidine bases in nucleic acids, and also present in a number of drugs, including those with anticancer, antiviral, antibacterial and antihypertensive activities.[1,2] Another important application of aromatic strongly electron-withdrawing pyrimidine moiety is the construction of push-pull molecules and the synthesis of functionalized π-conjugated materials such as liquid crystals, light-emitting, and nonlinear optical materials.[3] The pyrimidine-based structures, containing simultaneously pharmacophore and fluorophore, are justifiably appealing for the development of bioimaging probes.[4]

On contrary, pyrimidine *N*-oxides have been less investigated and found very few applications in pharmaceuticals or material sciences. The only clinical drug containing this scaffold is Minoxidil, an antihypertensive vasodilator medication used to treat hair loss.[5] Nevertheless, heterocyclic *N*-oxides possess their specific modes of action and represent highly challenging structures for drug-development.[6] The use of pyrimidine *N*-oxides for construction of extended π-conjugated systems is not described either, despite having large electron-withdrawing effect and dipole moment, which is significantly higher than that of pyrimidines'.[7] The most evident cause of such oversight is the lack of straightforward and selective synthetic approaches to pyrimidine *N*-oxides and their functional derivatives.

Scheme 1

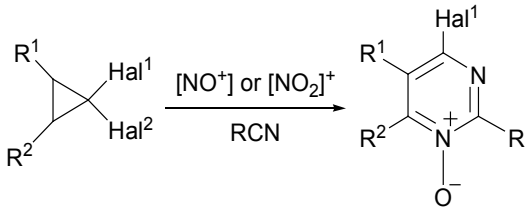

Previously, we have discovered a three-component heterocyclization of 1,1-dihalogenocyclopropanes upon the treatment with nitrating or nitrosating reagents in the presence of an organic nitrile affording 4-halogenopyrimidine oxides (Scheme 1). Additionally, we elaborated approaches to a number of pyrimidine derivatives based on this reaction.[8]

Here we present the synthetic approach to novel π-conjugated molecules based on pyrimidine *N*-oxide moiety and the investigation of their photophysical properties and anticancer activity.

2. Materials and methods

2.1. Experimental

General. Heterocycles **1a,b**,[8a,c] **2a-c**,[8d] **5**[8d] were obtained via described methods, synthesis and characterisation of novel intermediate compounds **1c, 2d-f** are available in SI. All starting materials were commercially available. All reagents except commercial products of satisfactory quality were purified according to literature procedures prior to use. Analytical thin layer chromatography was carried out with silica gel plates (supported on aluminum); the detection was done by UV lamp (254 and 365 nm). Column chromatography was performed on silica gel (Merck, 230–400 mesh). ^{1}H, ^{13}C and ^{19}F NMR spectra were recorded on a 400 MHz spectrometer (400.0, 100.6 and 376.3 MHz for ^{1}H, ^{13}C and ^{19}F, respectively) at room temperature; chemical shifts were measured with reference to the solvent for ^{1}H ($CDCl_3$, δ = 7.24 ppm) and ^{13}C ($CDCl_3$, δ = 77.13 ppm) and to $CFCl_3$ as external standard for ^{19}F. When necessary, assignments of signals in NMR spectra were made using 2D techniques. Accurate mass measurements (HRMS) were obtained with electrospray ionization (ESI) and a time-of-flight (TOF) detector. Ultraviolet/Visible spectra were obtained on Agilent Cary 60 spectrophotometer. Fluorescence spectra in solutions were recorded on Hitachi F2700 fluorescence spectrophotometer. Fluorescence spectrum of **3a** in thin film was recorded on Fluoromax4 fluorescence spectrophotometer. Fluorescence quantum yield (±10%) determined relative to quinine sulfate in 0.05 M H_2SO_4 (ψ = 53%) and rodamine-G in ethanol for **3o** (ψ = 94%) as standards.[9] Fluorescence intensity decays were obtained by time-correlated single photon-counting measurements in CH_2Cl_2 at 25 °C at c

≈ 10^{-5} M. Excitation wavelength – 370 nm. Typical fluorescence intensity decay data were analyzed by the Marquardt–Levenberg method of nonlinear fitting of one-, two- or three-exponential function (as a sum of discrete exponential terms); in the cases of **3a,o,q** not monoexponential intensity decay was observed.

2.2. Synthesis

Condensation of 4-aminopyrimidine oxides with aldehydes in basic conditions (general method). A mixture of 4-aminopyrimidine *N*-oxide **2** (0.5 mmol), corresponding aldehyde (1.0 mmol), 50% aqueous NaOH (2 g, 0.05 mol) and TEBAC (5 mg, 0.02 mmol) was stirred for 1–6 h under argon at 90–100ºC. After this time, the reaction mixture was allowed to cool down, diluted with water (5 mL) and extracted with CH_2Cl_2 (4 × 5 mL). The combined organic extracts were washed with water (3 × 5 mL) and dried over $MgSO_4$. The solvent was evaporated in vacuo and the product was isolated via the column chromatography (SiO_2).

Compound 3a was synthesized according to the general procedure (reaction time 1 h) from **2a** and benzaldehyde in 20% isolated yield. Yellow crystals, mp 185–188 °C (from CH_2Cl_2), R*f* 0.3 (petroleum ether:EtOAc:MeOH 1:1:0.2). ^{1}H NMR (400.0 MHz, $CDCl_3$) δ_H: 1.65–1.75 (2H, m, C^6H_2), 1.85–1.95 (2H, m, C^7H_2), 2.59 (2H, m, C^5H_2), 2.97 (m, 2H, C^8H_2), 3.31–3.38 (4H, m, 2 CH_2N), 3.81–3.90 (4H, m, $2CH_2O$), 7.29–7.39 (3H, m, 3CH, Ph), 7.62–7.68 (2H, m, 2CH, Ph), 7.90 (1H, br.d, *J* = 16.2 Hz, CH=), 7.99 (1 H, d, *J* = 16.2 Hz, CH=); ^{13}C NMR (100.6 MHz, $CDCl_3$) δ_C: 21.4 (C^7H_2), 21.7 (C^6H_2), 25.5 (CH_2), 26.3 (CH_2), 49.0 ($2CH_2N$), 66.7 ($2CH_2O$), 117.9 (CH=), 119.8 (C^{4a}), 127.9 (2CH, Ph), 128.7 (2CH, Ph), 129.3 (CH, Ph), 136.2 (C, Ph), 139.2 (CH=), 151.2 (C^2), 154.5 (C^4), 155.9 (C^{8a}). Found: $[M+H]^+$ 338.1860; molecular formula $C_{20}H_{23}N_3O_2$ requires $[M+H]^+$ 338.1863.

Compound 3b was synthesized according to the general procedure (reaction time 3 h) from **2a** and 2,6-dimethylbenzaldehyde in 32% isolated yield. Yellow crystals, mp 162–164 °C (from CH_2Cl_2), R*f* 0.3 (petroleum ether:EtOAc:MeOH 1:1:0.2). ^{1}H NMR (400.0 MHz, $CDCl_3$) δ_H: 1.66–1.74 (2H, m, CH_2), 1.86–1.95 (2H, m, CH_2), 2.42 (6H, s, $2CH_3$), 2.58 (2H, m, CH_2),

2.95 (2H, m, CH_2), 3.30–3.38 (4H, m, $2CH_2N$), 3.80–3.88 (4H, m, $2CH_2O$), 7.03–7.12 (3H, m, 3CH, Ar), 7.59 (1H, d, J = 16.5 Hz, CH=), 8.08 (1H, d, J = 16.5 Hz, CH=); ^{13}C NMR (100.6 MHz, $CDCl_3$) δ_C: 21.3 ($2CH_3$), 21.4 (CH_2), 21.7 (CH_2), 25.4 (CH_2), 26.3 (CH_2), 49.0 ($2CH_2N$), 66.7 ($2CH_2O$), 119.8 (C^{4a}), 123.0 (CH=), 127.7 (CH, Ar), 128.2 (2CH, Ar), 135.3 (C, Ar), 136.8 (2C, Ar), 137.6 (CH=), 151.2 (C^2), 154.4 (C^4), 155.9 (C^{8a}). Found: $[M+H]^+$ 366.2170; molecular formula $C_{22}H_{27}N_3O_2$ requires $[M+H]^+$ 366.2176.

Compound 3c was synthesized according to the general procedure (reaction time 5 h) from **2a** and 4-methylbenzaldehyde in 25% isolated yield. Yellow crystals, mp 203–206 °C (from CH_2Cl_2), R*f* 0.3 (petroleum ether:EtOAc:MeOH 1:1:0.2). ^{1}H NMR (400.0 MHz, $CDCl_3$) δ_H: 1.65–1.75 (2H, m, C^6H_2), 1.86–1.96 (2H, m, C^7H_2), 2.58 (2H, m, C^5H_2), 2.95 (2H, m, C^8H_2), 3.02 (6H, s, $2CH_3$, NMe_2), 3.30–3.36 (4H, m, $2CH_2N$), 3.83–3.89 (4H, m, $2CH_2O$), 6.66–6.72 (2H, m, 2CH, Ar), 7.53–7.60 (2H, m, 2CH, Ar), 7.79 (1H, d, J = 16.1 Hz, CH=), 7.87 (d, 1H, J = 16.1 Hz, CH=); ^{13}C NMR (100.6 MHz, $CDCl_3$) δ_C: 21.5 (C^7H_2), 21.7 (C^6H_2), 25.6 (C^8H_2), 26.1 (C^5H_2), 40.2 ($2CH_3$), 49.0 ($2CH_2N$), 66.8 ($2CH_2O$), 111.9 (2CH), 112.7 (=CH), 118.5 (C^{4a}), 124.3 (C, Ar) 129.5 (2CH), 139.7 (=CH), 151.1 (C, Ar), 152.0 (C^2), 154.5 (C^4), 155.5 (C^{8a}). Found: $[M+H]^+$ 381.2285; molecular formula $C_{22}H_{28}N_4O_2$ requires $[M+H]^+$ 381.2285.

Compound 3d was synthesized according to the general procedure (reaction time 6 h) from **2a** and 4-methoxybenzaldehyde in 27% isolated yield. Yellow crystals, mp 171–172 °C (from CH_2Cl_2), R*f* 0.3 (petroleum ether:EtOAc:MeOH 1:1:0.2). ^{1}H NMR (400.0 MHz, $CDCl_3$) δ_H: 1.63–1.76 (2H, m, C^6H_2), 1.84–1.94 (2H, m, C^7H_2), 2.57 (2H, m, C^5H_2), 2.96 (2H, m, C^8H_2), 3.31–3.39 (4H, m, $2CH_2N$), 3.80–3.87 (4H, m, $2CH_2O$), 3.83 (3H, s, CH_3), 6.87–6.93 (m, 2H, 2CH, Ar), 7.57–7.63 (2H, m, 2CH, Ar), 7.84 (1H, d, J = 16.2 Hz, CH), 7.87 (1H, d, J = 16.2 Hz, CH=); ^{13}C NMR (100.6 MHz, $CDCl_3$) δ_C: 21.4 (C^7H_2), 21.7 (C^6H_2), 25.5 (C^8H_2), 26.3 (C^5H_2), 49.0 ($2CH_2N$), 55.3 (CH_3), 66.7 ($2CH_2O$), 114.2 (2CH), 115.4 (=CH), 119.2 (C^{4a}),

128.9 (C, Ar) 129.5 (2CH), 139.2 (=CH), 151.6 (C^2), 154.8 (C^4), 155.8 (C^{8a}), 160.7 (C, Ar). Found: $[M+H]^+$ 368.1962; molecular formula $C_{21}H_{25}N_3O_3$ requires $[M+H]^+$ 368.1969.

Compound 3e was synthesized according to the general procedure (reaction time 6 h) from **2a** and 4-ethoxybenzaldehyde in 25% isolated yield. Yellow crystals, mp 166-169°C (from CH_2Cl_2), R*f* 0.2 (petroleum ether:EtOAc:MeOH 1:1:0.2). ^{1}H NMR (400.0 MHz, $CDCl_3$) δ_H: 1.41 (3H, t, *J* = 7.0 Hz, CH_3), 1.61–1.76 (2H, m, C^6H_2), 1.83–1.94 (2H, m, C^7H_2), 2.57 (2H, m, C^5H_2), 2.95 (2H, m, C^8H_2), 3.26–3.38 (4H, m, $2CH_2N$), 3.79–3.88 (4H, m, $2CH_2O$), 4.05 (2H, q, *J* = 7.0 Hz, CH_2, Et), 6.88 (2H, d, *J* = 8.6 Hz, 2CH), 7.58 (2H, d, *J* = 8.6 Hz, 2CH), 7.85 (2H, d, *J* = 16.2 Hz, 2CH=). ^{13}C NMR (100.6 MHz, $CDCl_3$) δ_C: 14.8 (CH_3), 21.4 (C^6H_2), 21.7 (C^7H_2), 25.5 (C^8H_2), 26.2 (C^5H_2), 49.0 ($2CH_2N$), 63.5 (CH_2, Et), 66.7 ($2CH_2O$), 114.7 (2CH, Ar), 115.4 (CH=), 119.3 (C^{4a}), 128.8 (C), 129.5 (2CH, Ar), 139.0 (CH=), 151.5 (C^2), 154.6 (C^4), 155.8 (C^{8a}), 160.1 (C, Ar). Found: $[M+H]^+$ 382.2116; molecular formula $C_{22}H_{27}N_3O_3$ requires $[M+H]^+$ 382.2125.

Compound 3f was synthesized according to the general procedure (reaction time 6 h) from **2a** and 3,4,5-trimethoxybenzaldehyde in 15% isolated yield. Yellow crystals, mp 162–165 °C (from CH_2Cl_2), R*f* 0.16 (petroleum ether:EtOAc:MeOH 1:1:0.2). ^{1}H NMR (400.0 MHz, $CDCl_3$) δ_H: 1.67–1.73 (2H, m, C^6H_2), 1.85–1.96 (2H, m, C^7H_2), 2.58 (2H, m, C^5H_2), 2.95 (2H, m, C^8H_2), 3.29–3.38 (4H, m, $2CH_2N$), 3.82–3.87 (4H, m, $2CH_2O$), 3.87 (3H, s, CH_3), 3.89 (6H, s, $2CH_3$), 6.87 (2H, s, 2CH), 7.80 (1H, d, *J* = 16.0 Hz, CH=), 7.91 (1H, d, *J* = 16.0 Hz, CH=); ^{13}C NMR (100.6 MHz, $CDCl_3$) δ_C: 21.4 (C^6H_2), 21.7 (C^7H_2), 25.5 (C^8H_2), 26.3 (C^5H_2), 49.0 ($2CH_2N$), 56.2 ($2CH_3$), 60.9 (CH_3), 66.7 ($2CH_2O$), 105.0 (2CH), 117.2 (CH=), 119.8 (C^{4a}), 131.8 (C, Ar), 139.1 (CH=), 139.3 (C, Ar), 151.1 (C^2), 153.4 (2C, Ar), 154.6 (C^4), 155.9 (C^{8a}). Found: $[M+H]^+$ 428.2169; molecular formula $C_{23}H_{29}N_3O_5$ requires $[M+H]^+$ 428.2180.

Compound 3g was synthesized according to the general procedure (reaction time 6 h) from **2a** and 4-(diethoxymethyl)benzaldehyde. Was not isolated because of transformation into **3h** on silica gel. ^{1}H NMR (400.0 MHz, $CDCl_3$) δ_H: 1.25 (6H, t, *J* = 6.8 Hz, $2CH_3$), 1.69–1.77

(2H, m, C^6H_2), 1.88–1.97 (2H, m, C^7H_2), 2.60 (2H, m, C^5H_2), 3.00 (2H, m, C^8H_2), 3.33–3.44 (4H, m, $2CH_2N$), 3.51-3.69 (4H, m, $2CH_2$, Et), 3.83–3.91 (4H, m, CH_2O), 5.52 (1H, s, CH), 7.50 (2H, d, *J* = 8.2 Hz, 2CH, Ar), 7.66 (2H, d, *J* = 8.2 Hz, 2CH), 7.92 (1H, d, *J* = 15.9 Hz, CH), 7.98 (1H, d, *J* = 15.9 Hz, CH).

Compound 3h was obtained from compound **3g** after the column chromatography in 12% isolated yield (per starting compound **2a**). Orange crystals, mp 186–188 °C (from CH_2Cl_2), R*f* 0.5 (petroleum ether:EtOAc:MeOH 1:1:0.4). ^{1}H NMR (400.0 MHz, $CDCl_3$) δ_H: 1.66–1.74 (2H, m, C^6H_2), 1.88–1.95 (2H, m, C^7H_2), 2.59 (2H, m, C^5H_2), 2.95 (2H, m, C^8H_2), 3.29–3.38 (4H, m, $2CH_2N$), 3.79–3.89 (4H, m, $2CH_2O$), 7.78 (2H, d, *J* = 8.1 Hz, 2CH), 7.88 (2H, d, *J* = 8.1 Hz, 2CH), 7.92 (1H, d, *J* = 16.1 Hz, CH=), 8.10 (1H, d, *J* = 16.1 Hz, CH=), 10.0 (1H, s, CHO); ^{13}C NMR (100.6 MHz, $CDCl_3$) δ_C: 21.3 (C^7H_2), 21.6 (C^6H_2), 25.5 (C^8H_2), 26.3 (C^5H_2), 49.0 ($2CH_2N$), 66.7 ($2CH_2O$), 120.7 (C^{4a}), 121.2 (=CH), 128.3 (2CH, Ar), 130.1 (2CH, Ar), 136.3 (C, Ar), 137.3 (=CH), 142.0 (C, Ar), 150.5 (C^2), 154.5 (C^4), 156.1 (C^{8a}), 191.6 (CHO). Found: $[M+H]^+$ 366.1811; molecular formula $C_{21}H_{23}N_3O_3$ requires $[M+H]^+$ 366.1812.

Compound 3i was synthesized according to the general procedure (reaction time 2 h) from **2a** and *trans*-4-stilbenecarboxaldehyde in 25% isolated yield. Yellow crystals, mp 188–191 °C (from CH_2Cl_2), R*f* 0.2 (petroleum ether:EtOAc:MeOH 1:1:0.2). ^{1}H NMR (400.0 MHz, $CDCl_3$) δ_H: 1.65–1.74 (2H, m, C^6H_2), 1.85–1.95 (2H, m, C^7H_2), 2.59 (2H, m, C^5H_2), 2.98 (2H, m, C^8H_2), 3.32–3.40 (4H, m, $2CH_2N$), 3.81–3.89 (4H, m, $2CH_2O$), 7.09 (1H, d, *J* = 16.3 Hz, =CH), 7.16 (1H, d, *J* = 16.3 Hz, CH), 7.23–7.28 (1H, m, CH), 7.32–7.38 (2H, m, 2CH), 7.48–7.55 (4H, m, 4CH), 7.65 (2H, d, *J* = 8.3 Hz, 2CH), 7.90 (1H, d, *J* = 16.1 Hz, =CH), 8.01 (1H, d, *J* = 16.1 Hz, =CH); ^{13}C NMR (100.6 MHz, $CDCl_3$) δ_C: 21.4 (C^7H_2), 21.7 (C^6H_2), 25.6 (C^8H_2), 26.4 (C^5H_2), 49.0 ($2CH_2N$), 66.7 ($2CH_2O$), 117.5 (CH=), 119.6 (C^{4a}), 126.6 (2CH), 126.9 (2CH), 127.8 (CH, Ph), 128.0 (CH=), 128.4 (2CH), 128.7 (2CH), 129.5 (CH=), 135.4 (C), 137.1 (C), 138.4 (C), 138.9 (CH=), 151.4 (C^2), 154.9 (C^4), 156.0 (C^{8a}). Found: $[M+H]^+$ 440.2324; molecular formula $C_{28}H_{29}N_3O_2$ requires $[M+H]^+$ 440.2333.

Compound 3j was synthesized according to the general procedure (reaction time 2 h) from **2b** and benzaldehyde in 17% isolated yield. Yellow oil, R_f 0.24 (petroleum ether: CH_2Cl_2:MeOH 3:1:0.1). ^{1}H NMR (400.0 MHz, $CDCl_3$) δ_H: 1.01 (3H, t, J = 7.3 Hz, CH_3), 1.46 (2H, m, CH_2, Bu), 1.67 (2H, m, CH_2, Bu), 1.73-1.86 (4H, m, C^6H_2, C^7H_2), 2.35 (2H, m, C^5H_2), 2.95 (2H, m, C^8H_2), 3.58 (2H, td, J = 7.0 Hz, J = 5.7 Hz, CH_2NH), 4.54 (1H, br.s, NH), 7.30-7.34 (1H, m, CH, Ph), 7.36-7.40 (2H, m, 2CH, Ph), 7.67 (2H, m, 2CH, Ph), 7.92 (1H, d, J = 16.1 Hz, CH=), 8.04 (d, 1H, J = 16.1 Hz, CH=); ^{13}C NMR (100.6 MHz, $CDCl_3$) δ_C: 13.9 (CH_3), 20.2 (CH_2, Bu), 20.9 (C^7H_2), 21.1 (C^6H_2), 22.4 (C^5H_2), 24.6 (C^8H_2), 31.6 (CH_2, Bu), 41.0 (CH_2N), 112.8 (C^{4a}), 118.3 (CH=), 127.9 (2CH, Ph), 128.3 (CH, Ph), 128.7 (2CH, Ph), 136.4 (C, Ph), 138.8 (CH=), 151.3 (C^4), 151.4 (C^2), 153.4 (C^{8a}). Found: $[M+H]^+$ 324.2068; molecular formula $C_{20}H_{25}N_3O$ requires $[M+H]^+$ 324.2070.

Compound 3k was synthesized according to the general procedure (reaction time 3 h) from **2c** and benzaldehyde in 21% isolated yield**.** Brown oil, R*f* 0.2 (petroleum ether:EtOAc:MeOH 1:1:0.2). ^{1}H NMR (400.0 MHz, $CDCl_3$) δ_H: 1.85–1.90 (4H, m, C^6H_2, C^7H_2), 2.56 (2H, m, C^5H_2), 3.00 (2H, m, C^8H_2), 7.12–7.18 (2H, m, 2CH), 7.21-7.27 (1H, m, 1CH), 7.32-7.42 (4H, m, 4CH), 7.59-7.66 (3H, m, 3CH), 7.88 (1H, d, J = 16.0 Hz, CH=), 7.94 (1H, d, J = 16.0, CH=); ^{13}C NMR (100.6 MHz, $CDCl_3$) δ_C: 20.8 (C^6H_2, C^7H_2), 22.8 (C^5H_2), 24.9 (C^8H_2), 114.1 (C^{4a}), 117.4 (CH=), 120.9 (2CH), 124.0 (CH), 128.1 (2CH), 128.8 (2CH), 128.9 (2CH), 129.6 (CH), 135.9 (C, Ph), 138.4 (CH), 140.6 (C, Ph), 151.9 (C), 152.1 (C), 154.9 (C^{8a}). Found: $[M+H]^+$ 344.1751; molecular formula $C_{22}H_{21}N_3O$ requires $[M+H]^+$ 344.1757.

Compound 3l was synthesized according to the general procedure (reaction time 3 h) from **2d** and benzaldehyde in 21% isolated yield**.** Brown crystals, mp 108–109 °C (from CH_2Cl_2), R_f 0.2 (petroleum ether: EtOAc:MeOH 1:1:0.3). ^{1}H NMR (400.0 MHz, $CDCl_3$) δ_H: 1.75–1.89 (4H, m, C^6H_2, C^7H_2), 2.50 (2H, m, C^5H_2), 2.93 (2H, m, C^8H_2), 3.81 (3H, s, CH_3), 6.53 (1H, s, NH), 6.88–6.93 (2H, m, 2CH, Ar), 7.26–7.37 (3H, m, 3CH, Ph), 7.47–7.52 (2H, m, 2CH, Ar), 7.55–7.59 (2H, m, 2CH, Ph), 7.81 (1H, d, J = 16.0 Hz, =CH), 7.97 (1H, d, J = 16.0

Hz, =CH); ^{13}C NMR (100.6 MHz, $CDCl_3$) δ_C: 20.9 (C^6H_2), 21.0 (C^7H_2), 22.7 (C^5H_2), 24.9 (C^8H_2), 55.5 (CH_3), 113.7 (C^{4a}), 114.0 (2CH, Ar), 117.9 (CH=), 122.8 (2CH, Ar), 127.9 (2CH, Ph), 128.7 (2CH, Ph), 129.2 (CH, Ph), 131.8 (C, Ar), 136.2 (C, Ph), 139.4 (CH=), 148.4 (C^4), 151.3 (C^2), 154.5 (C^{8a}), 156.1 (C, Ar). Found: $[M+H]^+$ 374.1852; molecular formula $C_{23}H_{23}N_3O_2$ requires $[M+H]^+$ 374.1863.

Compound 3m was synthesized according to the general procedure (reaction time 3 h) from **2a** and cinnamic aldehyde in 17% isolated yield**.** Yellow oil, R*f* 0.4 (petroleum ether:EtOAc:MeOH 1:1:0.1). ^{1}H NMR (400.0 MHz, $CDCl_3$) δ_H: 1.62–1.76 (2H, m, C^6H_2), 1.80–1.93 (2H, m, C^7H_2), 2.58 (2H, m, C^5H_2), 2.95 (2H, m, C^8H_2), 3.29–3.37 (4H, m, $2CH_2N$), 3.80–3.89 (4H, m, $2CH_2O$), 7.31–7.40 (4H, m, 3CH, Ph, CH=), 7.44–7.50 (1H, m, CH=), 7.62–7.67 (2H, m, 2CH, Ph), 7.89 (1H, ps.d, *J* = 16.3 Hz, CH=), 7.98 (1H, ps.d, *J* = 16.0 Hz, CH=); ^{13}C NMR (100.6 MHz, $CDCl_3$) δ_C: 21.4 (CH_2), 21.6 (CH_2), 25.5 (CH_2), 26.3 (CH_2), 49.0 ($2CH_2N$), 66.7 ($2CH_2O$), 117.8 (CH=), 119.7 (C^{4a}), 127.0 (CH=), 128.0 (2CH, Ph), 128.5 (CH=), 128.7 (2CH, Ph), 129.3 (CH, Ph), 136.1 (C, Ph), 139.3 (=CH), 151.2 (C^2), 154.7 (C^4), 156.0 (C^{8a}). Found: $[M+H]^+$ 364.2017; molecular formula $C_{22}H_{25}N_3O_2$ requires $[M+H]^+$ 364.2020.

Compound 3n was synthesized according to the general procedure (reaction time 2 h) from **2a** and 2-naphthaldehyde in 15% isolated yield**.** Orange crystals, mp 155-156 °C (from CH_2Cl_2), R*f* 0.4 (petroleum ether:EtOAc:MeOH 1:1:0.2). ^{1}H NMR (400.0 MHz, $CDCl_3$) δ_H: 1.63–1.75 (2H, m, C^6H_2), 1.83–1.94 (2H, m, C^7H_2), 2.58 (2H, m, C^5H_2), 2.97 (2H, m, C^8H_2), 3.30–3.42 (4H, m, $2CH_2N$), 3.80–3.90 (4H, m, $2CH_2O$), 7.46–7.51 (2H, m, 2CH, Ar), 7.53–7.57 (1H, m, 1CH, Ar), 7.82–7.86 (2H, m, 2CH, Ar), 7.96 (1H, d, *J* = 7.1 Hz, CH, Ar), 8.05 (1H, d, *J* = 15.8 Hz, CH=), 8.23 (1H, d, *J* = 8.4 Hz, CH, Ar), 8.78 (1H, d, *J* = 15.8 Hz, CH=); ^{13}C NMR (100.6 MHz, $CDCl_3$) δ_C: 21.4 (C^7H_2), 21.7 (C^6H_2), 25.5 (C^8H_2), 26.3 (C^5H_2), 49.0 ($2CH_2N$), 66.7 ($2CH_2O$), 120.0 (C^{4a}), 120.2 (CH=), 123.4 (CH, Ar), 124.9 (CH, Ar), 125.7 (CH, Ar), 125.9 (CH, Ar), 126.5 (CH, Ar), 128.7 (CH, Ar), 129.6 (CH, Ar), 131.5 (C, Ar), 133.3 (C,

Ar), 133.7 (C, Ar), 135.8 (CH=), 151.2 (C^2), 154.6 (C^4), 156.0 (C^{8a}). Found: $[M+H]^+$ 388.2010; molecular formula $C_{24}H_{25}N_3O_2$ requires $[M+H]^+$ 388.2020.

Compound 3o was synthesized according to the general procedure (reaction time 5 h; 0.7 eq. of aldehyde were taken instead of 2 eq.) from **2a** and perylene-3-carboxaldehyde in 10% isolated yield**.** Dark-red crystals, mp 155-156 °C (from CH_2Cl_2), R*f* 0.4 (petroleum ether:EtOAc:MeOH 1:1:0.4). ^{1}H NMR (400.0 MHz, $CDCl_3$) δ_H: 1.68–1.78 (2H, m, C^6H_2), 1.88–1.97 (2H, m, C^7H_2), 2.61 (2H, m, C^5H_2), 2.99 (2H, m, C^8H_2), 3.36–3.43 (4H, m, $2CH_2N$), 3.85–3.92 (4H, m, $2CH_2O$), 7.45–7.49 (2H, m, 2CH), 7.56 (1H, dd, *J* = 7.8, 8.4 Hz, CH), 7.65–7.69 (2H, m, 2CH), 7.98 (1H, d, *J* = 8.1 Hz, CH), 8.08 (1H, d, *J* = 15.7 Hz, =CH), 8.09 (1H, d, *J* = 8.4 Hz, CH), 8.22 (1H, d, *J* = 7.8 Hz, CH) 8.17–8.21 (3H, m, 3CH), 8.73 (1H, d, *J* = 15.7 Hz, =CH); ^{13}C NMR (100.6 MHz, $CDCl_3$) δ_C: 21.4 (C^7H_2), 21.7 (C^6H_2), 25.5 (C^8H_2), 26.3 (C^5H_2), 49.1 ($2CH_2N$), 66.8 ($2CH_2O$), 119.7 (=CH), 119.9 (C^{4a}), 120.3 (CH), 120.4 (CH), 120.6 (CH), 120.8 (CH), 123.1 (CH), 125.7 (CH), 126.6 (CH), 126.7 (CH), 126.9 (CH), 128.0 (CH), 128.2 (CH), 128.4 (C), 129.0 (C), 130.9 (C), 131.2 (C), 131.7 (C), 132.5 (C), 132.7 (C), 132.9 (C), 134.6 (C), 135.4 (=CH), 151.3 (C^2), 154.6 (C^4), 156.0 (C^{8a}). Found: $[M+H]^+$ 512.2326; molecular formula $C_{34}H_{29}N_3O_2$ requires $[M+H]^+$ 512.2333.

Compound 3p was synthesized according to the general procedure (reaction time 6 h) from **2a** and thiophene-2-carboxaldehyde in 12% isolated yield**.** Yellow crystals, mp 130–131 °C (from CH_2Cl_2), R*f* 0.2 (petroleum ether:EtOAc:MeOH 1:1:0.2). ^{1}H NMR (400.0 MHz, $CDCl_3$) δ_H: 1.64–1.75 (2H, m, C^6H_2), 1.86–1.94 (2H, m, C^7H_2), 2.57 (2H, m, C^5H_2), 2.94 (2H, m, C^8H_2), 3.29–3.36 (4H, m, $2CH_2N$), 3.81–3.86 (4H, m, $2CH_2O$), 7.03 (1H, dd, *J* = 3.7 Hz, *J* = 5.1 Hz, CH, Thio), 7.27 (1H, d, *J* = 3.7 Hz, CH, Thio), 7.32 (1H, d, *J* = 5.1 Hz, CH, Thio), 7.76 (1H, d, *J* = 15.8 Hz, CH=), 8.03 (1H, d, *J* = 15.8, CH=); ^{13}C NMR (100.6 MHz, $CDCl_3$) δ_C: 21.4 (C^7H_2), 21.7 (C^6H_2), 25.5 (C^8H_2), 26.2 (C^5H_2), 49.0 ($2CH_2N$), 66.7 ($2CH_2O$), 117.1 (CH=), 119.6 (C^{4a}), 127.4 (CH, Thio), 127.9 (CH, Thio), 129.2 (CH, Thio), 131.7 (CH=), 141.9 (C,

Thio), 150.9 (C^2), 154.5 (C^4), 155.8 (C^{8a}). Found: $[M+H]^+$ 344.1426; molecular formula $C_{18}H_{21}N_3O_2S$ requires $[M+H]^+$ 344.1427.

Compound 3q was synthesized according to the general procedure (reaction time 1 h; 10% aqueous NaOH (0.7 g, 17.5 mmol) was taken instead of 50%) from **2e** and benzaldehyde in 19% isolated yield**.** Yellow crystals, mp 195-198 °C (from CH_2Cl_2), R_f 0.6 (petroleum ether: EtOAc:MeOH 1:1:0.3). ^{1}H NMR (400.0 MHz, $CDCl_3$) δ_H: 3.66–3.73 (4H, m, $2CH_2N$), 3.79–3.89 (4H, m, $2CH_2O$), 6.50 (1H, s, C^5H), 7.31–7.41 (3H, m, 3CH, Ph), 7.42–7.49 (3H, m, 3CH, Ph), 7.63–7.68 (2H, m, 2CH, Ph), 7.74–7.78 (2H, m, 2CH, Ph), 7.93 (1H, d, J = 16.1 Hz, CH=), 8.03 (1H, d, J = 16.1 Hz, CH=); ^{13}C NMR (100.6 MHz, $CDCl_3$) δ_C: 44.6 ($2CH_2N$), 66.4 ($2CH_2O$), 102.1 (C^5H), 117.68 (CH=), 128.1 (2CH, Ph), 128.2 (2CH, Ph), 128.8 (2CH, Ph), 129.3 (2CH, Ph), 129.7 (CH, Ph), 130.2 (CH, Ph), 132.1 (C, Ph), 135.8 (C, Ph), 141.3 (CH=), 153.5 (C^4), 155.3 (C^2), 156.0 (C^6). Found: $[M+H]^+$ 360.1697; molecular formula $C_{22}H_{21}N_3O_2$ requires $[M+H]^+$ 360.1707.

Compound 3r was synthesized according to the general procedure (reaction time 1 h; 10% aqueous NaOH (0.7 g, 17.5 mmol) was taken instead of 50%) from **2e** and benzaldehyde in 18% isolated yield**.** Yellow crystals, mp 210-212 °C (from CH_2Cl_2), R_f 0.7 (petroleum ether: EtOAc:MeOH 1:1:0.2). ^{1}H NMR (400.0 MHz, $CDCl_3$) δ_H: 3.64–3.69 (4H, m, $2CH_2N$), 3.81–3.87 (4H, m, $2CH_2O$), 6.49 (1H, s, C^5H), 7.33–7.41 (3H, m, 3CH, Ph), 7.56–7.60 (2H, m, 2CH, C_6H_4Br), 7.63–7.67 (2H, m, 2CH, Ph), 7.69–7.73 (2H, m, 2CH, C_6H_4Br), 7.92 (1H, d, J = 16.1 Hz, CH=), 8.04 (1H, d, J = 16.1 Hz, CH=); ^{13}C NMR (100.6 MHz, $CDCl_3$) δ_C: 44.6 ($2CH_2N$), 66.4 ($2CH_2O$), 101.9 (C^5H), 117.7 (CH=), 124.7 (CBr), 128.1 (2CH, Ph), 128.8 (2CH, Ph), 129.6 (CH, Ph), 130.9 (2CH, C_6H_4Br), 131.1 (C, C_6H_4Br), 131.4 (2CH, C_6H_4Br), 135.8 (C, Ph), 140.8 (CH=), 152.5 (C^4), 154.2 (C^6), 154.9 (C^2). Found: $[M+H]^+$ 438.0821 and 440.0795; molecular formula $C_{22}H_{20}BrN_3O_2$ requires $[M+H]^+$ 438.0812 and 440.0792.

Compound 4 was obtained from *N*-oxide **3a** via described method[8b] in 95% isolated yield and required no purification**.** Yellowish crystals, mp 113–114 °C (from CH_2Cl_2). ^{1}H NMR

(400.0 MHz, $CDCl_3$) δ_H: 1.66–1.75 (2H, m, C^6H_2), 1.80–1.89 (2H, m, C^7H_2), 2.51 (2H, m, C^5H_2), 2.83 (2H, m, C^8H_2), 3.35–3.47 (4H, m, $2CH_2N$), 3.74–3.85 (4H, m, $2CH_2O$), 7.09 (1H, d, J = 16.0 Hz, =CH), 7.23–7.28 (1H, m, 1CH), 7.29–7.35 (2H, m, 2CH), 7.53–7.57 (2H, m, 2CH), 7.80 (1H, d, J = 16.0 Hz, CH); ^{13}C NMR (100.6 MHz, $CDCl_3$) δ_C: 22.3 (C^7H_2), 22.8 (C^6H_2), 26.7 (C^5H_2), 31.7 (C^8H_2), 48.6 ($2CH_2N$), 66.8 ($2CH_2O$), 116.4 (C^{4a}), 127.4 (2CH), 127.6 (CH=), 128.61 (CH), 128.64 (2CH), 136.3 (C, Ph), 136.5 (CH=), 160.1 (C^2), 164.2 (C^{8a}), 164.9 (C^4). Found: $[M+H]^+$ 322.1905; molecular formula $C_{20}H_{23}N_3O$ requires $[M+H]^+$ 322.1914.

2.3. X-ray analysis. For X-ray diffraction analysis was chosen single crystal of compound **3b**. Cell parameters for compound **3b** were determined from a set of 13467 reflections. Structure was solved by direct methods (*SHELXS97*),[10a] and refined with using anisotropic approximation for all nonhydrogen atoms. All hydrogen atoms were found from the different Fourier maps and refined with using riding model. Refinement procedure was made with using *SHELXL-13* program.[10b] The description and results of the single crystal experiment are given in Table S1. Graphical representations (Figure S1) of solved molecular structure was made with using *ORTEP-3* program.[10c] The CIF-file was checked (on-line procedure) by *PLATON*[10d] program and deposited in Cambridge Structural Data Base (deposit number 1545819). In the crystal structure classical hydrogen bonds are not found (Figure S2). By our opinion, crystal structure is stabilized by non-classical hydrogen bonds (Table S3) and intermolecular contacts (less than 4.00 Å) (Table S4).

2.4. Computational details

Molecular modelling, with Gaussian 09 and GaussView 5.0.8, was used to determine the HOMO and LUMO energies at the B3LYP/6-31G(d) was performed. The theoretical calculations for excitation and emission spectra were carried out using the Gaussian 09 implementations of B3LYP DFT. Using the optimized geometries in CH_2Cl_2 (PCM model), vertical transitions in the UV−vis region were computed with time-dependent DFT (TDDFT) to

generate the simulated absorption spectra. For TDDFT single points, the first 6 (for **3o** NState = 20) singlet excitations were solved iteratively [TD(ROOT = X, NSTATES = 6) where X is the root number, X = 1]. For TDDFT geometry optimizations, the first singlet excited states were optimized using analytical gradients, and the first 6 singlet excitations were solved iteratively [TD(ROOT = 1, NSTATES = 6)]. All Gaussian 09 computations used the 6-31G(d) basis sets for all atoms. Spherical harmonic d functions were used throughout, i.e., there are five angular basis functions per d function. All B3LYP/6-31G(d) structures were fully optimized, and analytical frequency calculations were performed on all ground-state structures to ensure a local minimum was achieved.

2.5. Bioevaluation

MTT test. The MTT test of compounds **3a-f,h,i,m-o** was performed according to the described procedure[11] with small modifications. MCF7, HCT116 human cancer cell lines were cultured in DMEM (PanEco, Russia) with Glutamin (PanEco, Russia) and antibiotics (PanEco, Russia) in CO2 (5%) at 37°C. The compounds were predissolved (20 mM) in DMSO and then added to the cell-culture medium at the required concentration with a maximum DMSO content of 0.5 v/v-%. At these concentrations, DMSO has no effect on cell viability, as it was shown in control experiments. Cells were cultured in 96-well plates (7000 cells/well) and treated with various concentrations of the title compounds (from 0.01 to 50 μM) as well as doxorubicin at 37 °C for 72 h. Cell viability was determined by using the MTT assay, which quantifies the mitochondrial activity. Then, the cells were incubated at 37 °C for 50 min with a solution of MTT, 3-(4,5-dimethylthiazol-2-yl)-2,5-diphenyltetrazolium bromide (10 μL, 5 $mg \times mL^{-1}$) (Sigma-Aldrich, St. Louis, USA). The supernatant was discarded, and cells were dissolved in DMSO (100 μL). The optical density of the solution was measured at 570 nm with use of a multiwall-plate reader (Anthos Zenyth 2000rt, Biochrom, Great Britain,), and the percentage of surviving cells was calculated from the absorbance of untreated cells. Each experiment was repeated at least three times, and each concentration was tested in at least three replicates. Data

were presented as (relative cell growth inhibition) a graph of the percentage of surviving cells versus the concentration of the test substances (Figure S4). The meanings of 50% inhibition concentration (IC_{50}) were performed with standard deviation.

Cell toxicity assay. The citotoxicity of compounds **3a,c,e,f,i,j,l,n,q,r** was evaluated according to the described procedure.[12a] The porcine embryo kidney (PEK) cell line were seeded and incubated at 37°C for 72 h in 96-well plates. Stock solutions of the studied compounds with a concentration of 5 mM were prepared in 100% DMSO and two-fold dilutions were prepared in medium 199 in Earle solution to obtain final concentrations starting from 50 μM. Equal volumes of compound dilutions were added in four replicates to the cells. Control cells were treated with the same sequential concentrations of DMSO, as in compound dilutions in four replicates in the same medium. After incubation at 37°C on days 1 or 7, the morphology of the cells was visualized with the microscope and CC_{50} values were calculated according to the Kerber method.[12b]

Cell uptake behavior. The cell uptake behavior of compounds **3a** and **3n** was examined by a microscope Axioplan 2 imaging MOT (Carl Zeiss, Germany) with a digital camera AxioCam Hrc (Carl Zeiss); photos were processed with AxioVision 4.5 soft (Carl Zeiss). HCT116 and MCF7 cells cultures (5×10^4 cells per mL) were used. The fluorescence was excited by a mercury lamp with FRET CFP filters (Filter set 48 FRET CFP/YFP shift free; EX BP 436/20, BS FT 455, EM BP 535/30). The cells were cultivated in flasks 72, unhitched and suspended in DMEM. Compounds **3a** or **3n** in concentrations 25 or 250 μM were incubated with cells for 1 h at 25 °C. Afterward, the cells were washed two times with DMEM and the photos were obtained (Figures 6, S6,7).

Synthetic details, characterisation of novel starting and intermediate compounds **1c, 2d-f**, details of X-ray data collection and structure refinement, details of bioevaluation, copies of absorption and emission spectra, computational details, copies of NMR spectra are available in SI.

3. Results and discussions

Two main synthetic transformations were used for the approach to previously unknown π-conjugated systems: i) S_NAr reactions in electron-deficient pyrimidine oxide system and ii) the Knoevenagel-type condensation, employing methyl group in the position *2* of heteroaromatic ring.[13] It should be noted that in contrast with pyrimidines, the reactivity of the oxidized heterocycles had not been studied systematically. There is only one described example with the use of 2-methylpyrimidine oxides' condensation with an aldehyde;[14a] along with several examples of the synthesis of 2-ethenyl derivatives of pyrimidine oxide *via* heterocyclization[14b-d] or oxidation.[14e] Furthermore, a limited number of examples of S_NAr reactions involving these compounds exists as well.[8d,14] Nevertheless, they definitely present promising substrates for such processes due to significant electron-withdrawing effect of the *N*-oxide moiety.[7a,16]

The series of pyrimidine *N*-oxides **2a-f** bearing alkyl- or arylamino group in position *4* were obtained from pyrimidine *N*-oxides **1a-c** under the treatment with corresponding nucleophiles (Scheme 2). The reactions proceeded smoothly in mild conditions.

Amino substituted pyrimidine *N*-oxide **2a** was studied in condensation with benzaldehyde (Scheme 2). The optimization of condensation conditions, including varying of basic or acidic catalyst, solvent and temperature (Table S1), was carried out and in all cases the condensation proceeded selectively at the methyl group. The best result was achieved when 50% aqueous NaOH was used as a base in the presence of TEBAC without organic solvent.

Under the optimized conditions, the series of novel pyrimidine *N*-oxides derivatives **3a-r** were obtained (Scheme 2). The aromatic aldehydes, containing electron donating substituents, were readily involved in the reaction with **2a** to give 2-arylidenepyrimidine *N*-oxides **3a-f,i-l**. Aldehydes containing the nitro-group or halogen atoms in the aryl moiety did not react with 2-methylpyrimidine *N*-oxides, and neither did acetophenone. The only condensation product containing an acceptor substituent in the styryl moiety that we obtained was compound **3h**. For this purpose, *N*-oxide **3g** was prepared as the precursor. As a bonus no additional synthetic

385 procedure was necessary because the acetal protective group was removed in the course of
386 column chromatography.

387 **Scheme 2**[a]

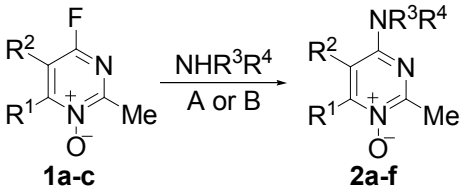

1a-c **2a-f**

2a, R^1-R^2 = -$(CH_2)_4$-, R^3-R^4 = -$(CH_2)_2O(CH_2)_2$-, 85% (A)
2b, R^1-R^2 = -$(CH_2)_4$-, R^3 = H, R^4 = Bu, 36% (A)
2c, R^1-R^2 = -$(CH_2)_4$-, R^3 = H, R^4 = Ph, 48% (B)
2d, R^1-R^2 = -$(CH_2)_4$-, R^3 = H, R^4 =(4-OMe-C_6H_4), 65% (B
2e, R^1=Ph, R^2 = H, R^3-R^4 = -$(CH_2)_2O(CH_2)_2$-, 62% (A)
2f, R^1=4-Br-C_6H_4, R^2 = H, R^3-R^4 = -$(CH_2)_2O(CH_2)_2$-, 56% (A)

1a, R^1-R^2 = -$(CH_2)_4$-; **1b**, R^1=Ph, R^2 = H; **1c**, R^1=4-Br-C_6H_4, R^2 = H

Conditions. **A**: morpholine or NH_2Bu as solvent, 24 h; **B**: NH_2Ph or NH_2(4-OMe-C_6H_4), DIPEA, EtOH, 1-7 days

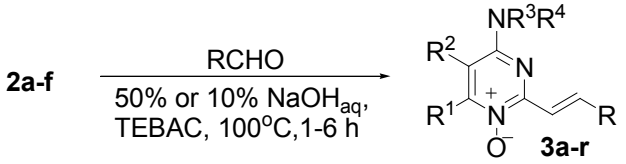

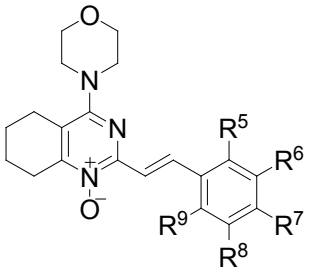

3a, R^5=R^6=R^7=R^8=R^9=H, 20%
3b, R^5=R^9=Me, R^6=R^7=R^8=H, 32%
3c, R^5=R^6=R^8=R^9=H, R^7=NMe_2, 25%
3d, R^5=R^6=R^8=R^9=H, R^7=OMe, 27%
3e, R^5=R^6=R^8=R^9=H, R^7=OEt, 25%
3f, R^5=R^9=H, R^6=R^7=R^8=OMe, 15%
3g, R^5=R^6=R^8=R^9=H, R^7=$CH(OEt)_2$[b]
3h, R^5=R^6=R^8=R^9=H, R^7=CHO, 12%[b]

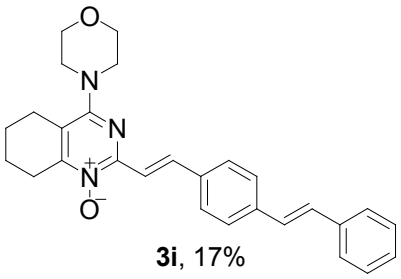

3i, 17%

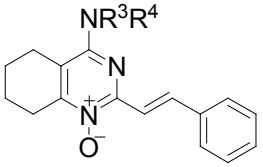

3j, R^3=H, R^4=Bu, 17%
3k, R^3=H, R^4=Ph, 21%
3l, R^3=H, R^4=4-(OMe)C_6H_4, 21%

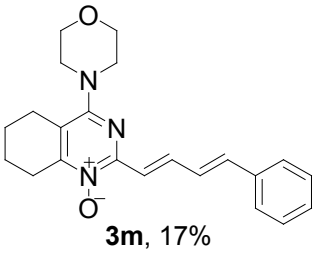

3m, 17%

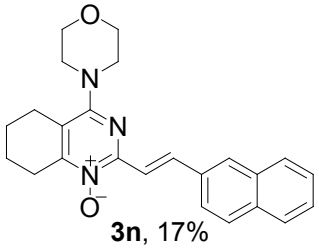

3n, 17%

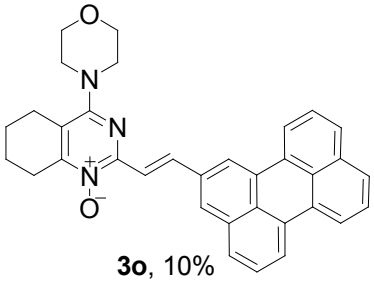

3o, 10%

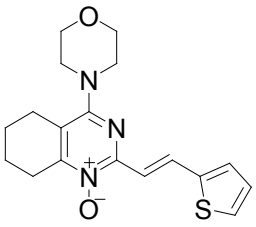

3p, 12%

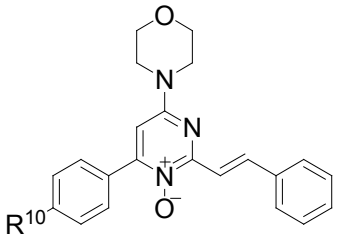

3q, R^{10}=H, 19%, **3r**, R^{10}=Br, 18%

388

389 [a]isolated yields; [b]acetal protective group of **3g** was removed on SiO_2 affording **3h**

390

391 The cinnamic aldehyde and aldehydes, containing naphtyl, perylenyl or thiophenyl
392 moieties, reacted with *N*-oxide **2a** affording compounds **3m-p** (Scheme 2). Pyrimidine *N*-oxides
393 **2e,f** were also involved into the reaction with benzaldehyde to give the heterocycles **3q,r** with

an additional aryl moiety in the pyrimidine ring (Scheme 2). Diluted solution of NaOH was used because the starting compounds were both more reactive and more labile than tetrahydroquinazoline derivatives **2a-d**.

The product of *N*-oxide reduction in compound **2a**, pyrimidine **5**, was also studied in condensation with benzaldehyde, but proved to be inert under the reaction conditions (Scheme 3). Therefore, a better pathway to compound **4** is the reduction of condensation product **3a**. Such a difference in reactivity of pyrimidines and more electron-withdrawing pyrimidine *N*-oxides have been previously observed[14a] and showed the significance of *N*-oxide electronic effects for the chemical behaviour of pyrimidine derivatives. Here, the comparison of **2a** and **5** in the condensation conditions demonstrates that the introduction of an *N*-oxide moiety into the molecule is sufficient to compensate for the deactivating effect of alkylamino group.

Scheme 3

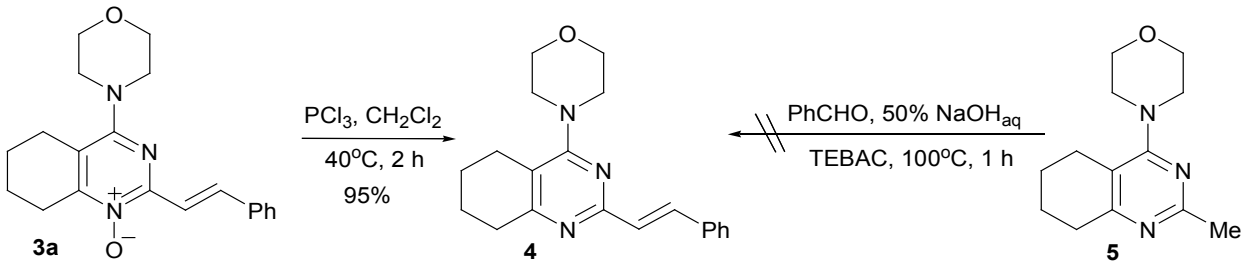

The photophysical properties of the obtained compounds were studied by UV-vis and fluorescence spectroscopy in CH_2Cl_2 at RT. Spectra of electronic absorption and emission were recorded; the absorption coefficients and fluorescence quantum yields were measured for all the obtained compounds (Figure 1, Table 1).

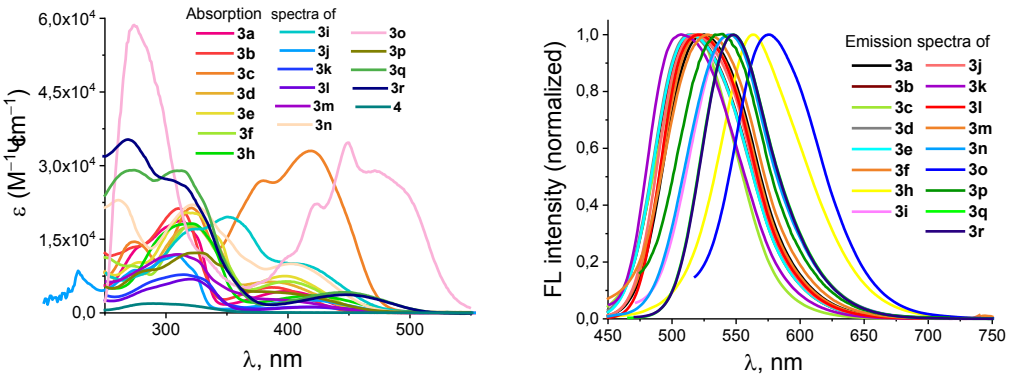

Figure 1. Electronic absorption (a) and fluorescence (b) spectra of **3a-r** in CH_2Cl_2 at RT.

Table 1. Photophysical properties of compounds **3a-r, 4**[a]

	λ^{max}_{abs}, nm[b]	λ^{max}_{em}, nm	$\Delta\lambda$, cm^{-1}	ε, $10^3 \cdot M^{-1} \cdot cm^{-1}$	ψ, %	τ, ns	μ, D[c]
3a	400	535[d]	6308	4.4	21	9.2	4.00
3b	384	536	7385	5.2	29	9.1	4.53
3c	420	523	4689	33.0	1.0	-	1.95
3d	391	533	6814	6.3	12	8.3	2.02
3e	384	515	6624	7.5	21	8.2	1.73
3f	390	521	6447	6.4	23	8.5	6.14
3h	418	565	6224	3.5	2.5	-	8.62
3i	406	531	5798	10.0	4	-	3.67
3j	415	520	4866	2.6	20	8.9	6.70
3k	416	508	4353	1.2	16	1.7 (6%) 10.3 (94%)	5.53
3l	420	520	4579	4.3	13	8.2	7.39
3m	400	546	6685	2.7	6	-	3.51
3n	400	546	6685	10.0	5	-	3.79
3o	470	575	3885	29.0	4	3.2 (69%) 5.4 (31%)	3.92
3p	400	534	6273	4.0	0.6	-	3.30
3q	445	548	4224	4.2	20	0.7 (25%) 2.5 (42%) 10.7 (33%)	4.26
3r	445	548	4224	3.7	15	3.7	4.93
4	284	333	5181	1.9	2.3	-	2.52

[a]All spectra were recorded in CH_2Cl_2 solutions at RT at c = (1.0−6.0) × 10^{-5} M. [b]The longest-wavelength absorption maxima. [c]Calculated dipole moments. [d]In solid state λ^{max}_{em} = 537 nm.

For most of the obtained compounds, the longest-wavelength absorption maxima are in the visible region, at 380–450 nm (Figure 1, Table 1). The most significant red-shift of maxima relative to compound **3a** (λ^{max}_{abs} = 400 nm) was achieved when the six-membered ring annelated to the pyrimidine moiety was substituted for aryl (**3q,r**, λ^{max}_{abs} = 445 nm), or when the perylenyl moiety was introduced into the molecule (**3o**, λ^{max}_{abs} = 470 nm). Strong absorption (ε over 10 $10^3 \cdot M^{-1} \cdot cm^{-1}$) in the long-wave region was demonstrated by compounds **3i,n,o**, containing the extended systems of conjugated bonds. The largest hyperchromic effect was observed when dimethylamino group was introduced in the structure (**3c**, ε = 33 $10^3 \cdot M^{-1} \cdot cm^{-1}$).

An interesting effect of structure on the absorption was observed for compound **3b**. Due to steric hindrance introduced by the *ortho*-methyl groups, the aryl ring is rotated out of the plane containing the pyrimidine moiety and double bond; whereas in **3a**, two phenyl rings lay in the

same plane, and more effective conjugation is achieved. As a result, λ^{max}_{abs} of dimethyl substituted compound **3b** is blueshifted comparing to **3a**. The molecular structure and geometry of **3b** were proved with DFT-calculations (for **3a,b**, Figure S3) and X-ray analysis (for **3b**, Figure S3).

π-Conjugated compounds **3a-r**, containing *N*-oxide moiety, were found to possess fluorescence properties in visible region. For compounds **3a-f**, either unsubstituted or bearing electron-donating groups in the aromatic ring, the emission maxima lay in the range of 515 to 536 nm (Figure 1, Table 1). However, introduction of an aldehyde function in *p*-position of the phenyl fragment (**3h**) redshifts the longest-wavelength emission maximum up to λ^{max}_{em} = 565 nm. For 4-alkyl and 4-arylamino *N*-oxides **3j-l** the emission maxima are blueshifted, and the Stokes shift is smaller. Unlike with **3a**, this is caused by less electron-donative properties of the substituents (i.e as compared with the dialkylamino group). Extension of the π-system (compounds **3i,m,n,q,r**) redshifts the emission maxima considerably, and this effect is the strongest for perylenyl substituted compound **3o**, giving λ^{max}_{em} = 575 nm. Replacement of phenyl with thiophenyl in **3p** slightly increases emission maximum, but the quantum yield becomes appreciably lower, possibly because of a more efficient intersystem crossing into the triplet state due to the heavy atom effect. For the compound **3a** it was shown that in solid state there was no shift of the emission maximum. Fluorescence lifetimes were measured for the compounds with the highest quantum yields, being in most cases 8-9 ns. A mono-exponential decrease in fluorescence was usually observed, but in some cases (especially if the molecule contained several aromatic rings) the dependence had a more complex form. Significant differences in fluorescence decay for **3q** and **3r** are apparently due to the presence of a bromine atom in the molecule.

Both the absorption and emission maxima of compound **4** were observed in UV region, being significantly blueshifted in comparison with its oxidized analogue **3a**. So, it can be

concluded that the presence of *N*-oxide group is essential for the absorption and fluorescence in the visible part of the spectrum.

To gain a deeper understanding of the electronic and photophysical properties of the synthesized compounds, we performed quantum-chemical simulations for **3a-r** and **4**. The FMO plots show that the HOMOs of the *N*-oxide molecules are mainly localized in the aminopyrimidine moiety, while LUMOs are localized through the whole conjugated system (Figure 2). Much less active charge-transfer is observed for deoxygenated analogue **4**, possessing strongly blueshifted absorption and emission maxima. The dipole moments of the molecules were also predicted, giving 1.6-8.7 D (Table 1), yet no correlation was found between them and photophysical properties of pyrimidine *N*-oxides. Computational details, FMO plots and energies, and comparison of experimental and calculated absorption and emission maxima wavelengths are given in SI.

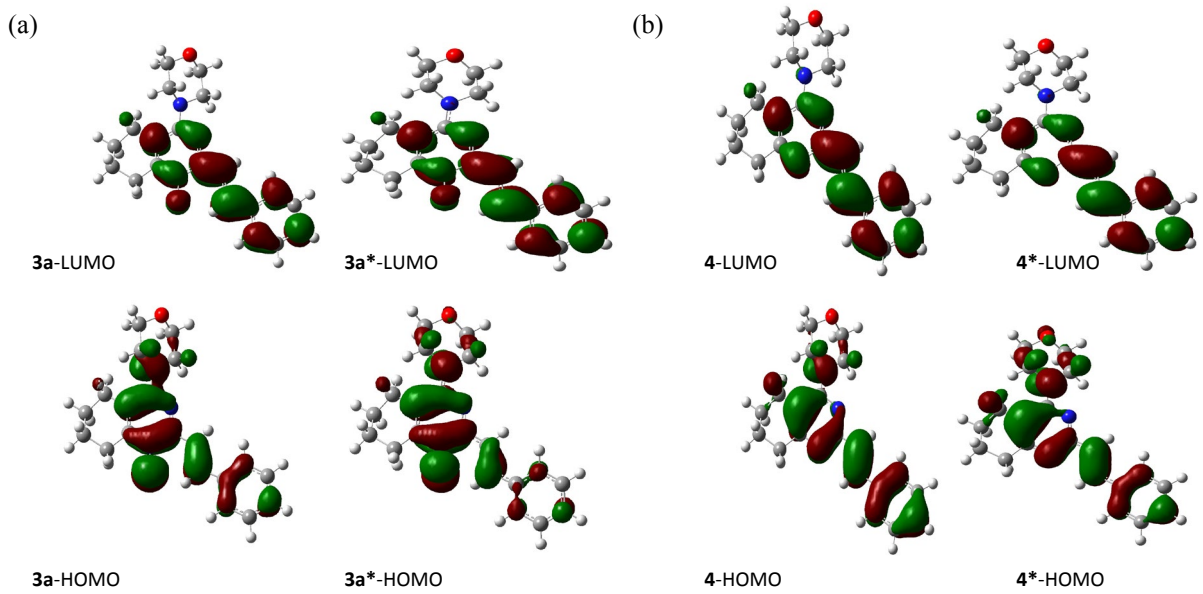

Figure 2. FMO plots (B3LYP/6-31G(d)) of (a) **3a** and (b) **4** in ground and excited states. FMO plots of **3b-r** are shown in Figures S10-S27 in the SI.

The investigated compounds possess solvatochromic effect, and for most of them, change in the emission color can be seen by the naked eye. Thus, for compound **3h**, changing the solvent from CH_2Cl_2 to methanol led to the change of fluorescence from yellow to green; that is presumably related to the formation of hydrogen bonds between carbonyl group and solvent molecules in methanol (Figure 3).

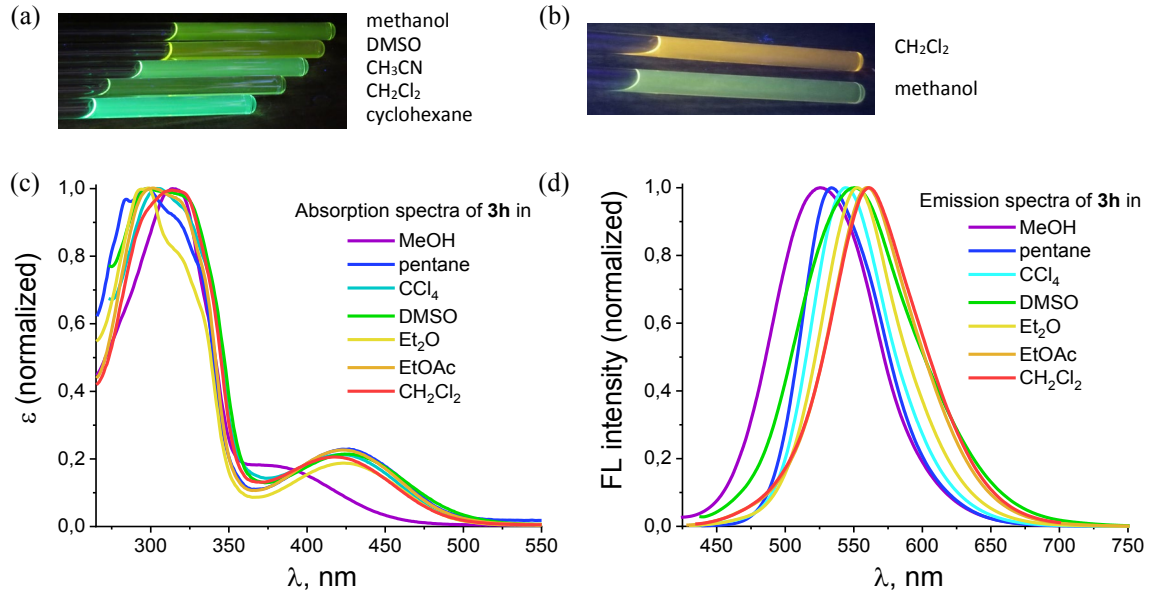

Figure 3. Fluorescence of **3a** (a) and **3h** (b); absorption (c) and emission (d) spectra of **3h** in different solvents at RT, $\lambda_{ex} = 365$ nm

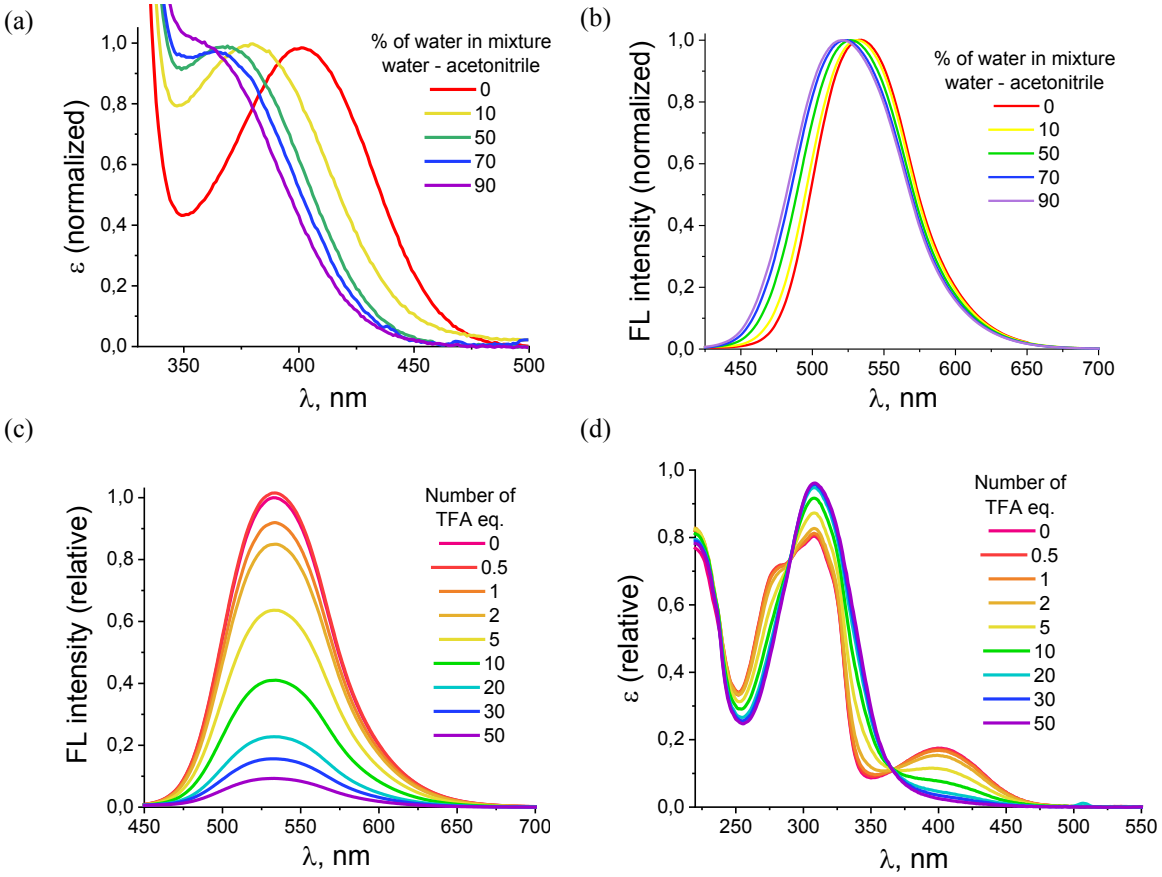

Figure 4. Electronic absorption and fluorescence spectral change of **3a** (2×10^{-5} mol L^{-1}) at RT (a,b) in CH_3CN–water mixtures with varying volumetric fractions of water; (c,d) in CH_2Cl_2 upon addition of TFA; $\lambda_{ex} = 400$ nm.

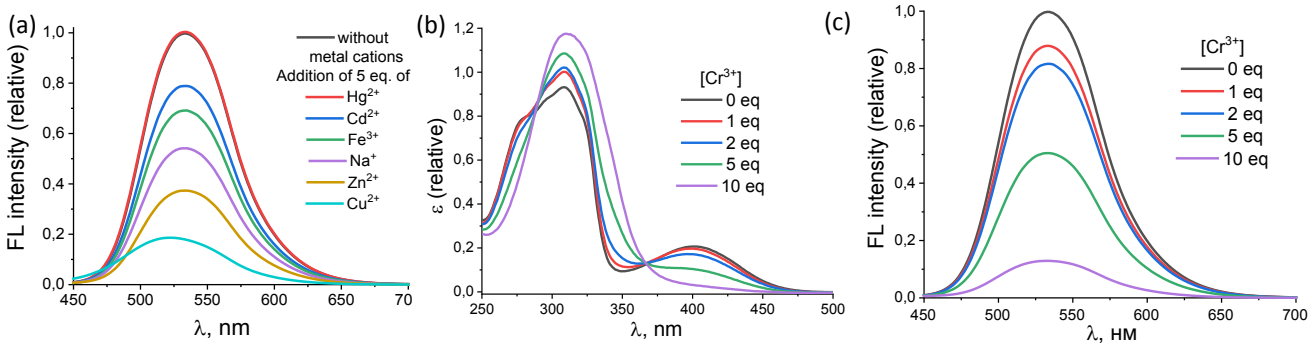

Figure 5. (a) Fluorescence spectra of **3a** (2×10^{-5} mol L^{-1}) upon addition of Hg^{1+}, Cd^{2+}, Fe^{3+}, Na^{+}, Zn^{2+} and Cu^{2+} (5 equiv.); (b,c) electronic absorption and fluorescence spectral change of **3a** (2×10^{-5} mol L^{-1}) upon addition of $Cr(ClO_4)_3$ in acetonitrile at RT; $\lambda_{ex} = 400$ nm.

Basing on their structure, the investigated compounds may be expected to exhibit aggregation-induced emission (AIE) feature.[17] In the search for the AIE effect, the emission spectra in CH_3CN–water with different volumetric ratios of water were recorded for the compound **3a**. It was shown (Figure 4a,b) that the increase of solvent polarity leads to the hypsochromic shift of absorption and emission maxima; yet neither AIE nor ACQ effects were observed.

For compound **3a**, the effect of the presence of acid in the medium on the absorption and fluorescence spectra was also studied. Upon addition of TFA, the absorption band at 400 nm disappeared and the solution of heterocycle became colorless. Fluorescent properties of **3a** were found to be sensitive to the medium pH: the protonation of the molecule led to fluorescence quenching (Figure 4c,d).

To probe the chemosensor properties of compound **3a**, its absorption and emission spectra were investigated in the presence of the metal cations in various concentrations (Figure 5). Analogous to the addition of acids, the addition of salts led to discoloration of the solution and significant quenching of fluorescence. There was no shift of wavelength maxima observed. The strongest changes were observed for Pb^{2+}, Cu^{2+}, Zn^{2+} ions, while Hg^{2+}, Ag^{+}, K^{+} ions showed almost no effect on absorption and emission (Figures 5, S9).

It should be mentioned that such behavior is not common for diazine fluorophores;[3a-c] the more common occurrence is the shift of emission bands upon protonation or complexation. Together with the

lack of fluorescence in deoxygenated compound **4** it probably indicates that the proton or metal ion binding involves the N-oxide, not the heterocyclic moiety. To prove this suggestion DFT calculations were performed for different protonated forms of **3a**, where a proton was either binded with a heteroatom or underwent an electrophilic addition to the C-C double bond. According to the calculations, the cationic form where the proton is binded with the oxygen atom lays 3.11 kcal/mol lower than the next alternative form. During such a protonation the FMOs of **3a** have changed to those revealing no charge-transfer and strongly resembling the corresponding FMOs in non-fluorescent compound **4** (Figures 2, S28). Speaking in terms of the electrons redistribution, the electron lone pair on oxygen of protonated **3a** is binded with a proton and cannot participate in charge-transfer on contrast to the free **3a**. The same effect can be assumed in the case of metals ions complexation that is to some extent confirmed by the pyrimidine *N*-oxides capability to bind with metals involving just oxygen, shown by X-ray analysis for the complex of **1a** with Cu^{2+}.[8a]

To evaluate potential applications of the obtained pyrimidine *N*-oxides as leading compounds for drug development and fluorescent dyes for biological imaging[18] we investigated their antiproliferative activity towards human cancer cells, toxicity and the cell uptake behavior.

The primary screening of biological activity of the series of morpholine-substituted π-conjugated molecules was completed. Compounds **3a-f,h,i,m-o** were evaluated for their antitumor potency against 2 types of human cancer cell lines: colon carcinoma HCT-116 and breast adenocarcinoma MCF7 (Table 2).

Table 2. IC_{50} values for cell viability found for compounds **3b,i,n** and doxorubicin (Dox) against cancer cell lines

Compounds	IC_{50}, μM	
	HCT-116	MCF7
3b	>50	28.7±8.4
3i	>50	11.7±4.3
3n	8.6±1.9	2.9±0.5
Dox	0.65±0.1	0.28±0.06

Three of these compounds showed moderate cytotoxic activity against the MCF7 cancer cell line (IC_{50} values for **3b,i,n** are below 50 μM), and the most active of them, compound **3n**, also demonstrated cytotoxicity towards the line HCT116 in micromolar concentration. Thus, in the studied series, the compound with the naphthalene moiety **3n** shows higher activity against both cell lines, which makes it the most promising candidate. This evaluation, though preliminary, reveals that introduction of hydrophobic sterically hindered substituents in position *2* is favorable for cytotoxicity.

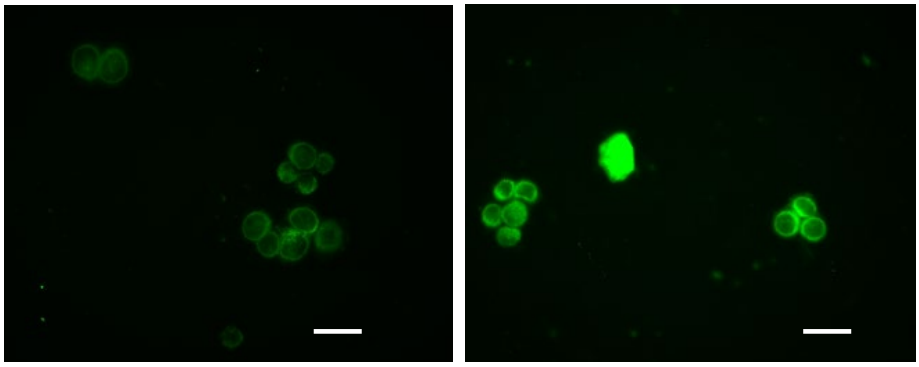

(a) (b)

Figure 6. Fluorescence of compound **3n** in MCF7 cells after incubation for 1 h. Concentration of **3n** was 25 μM (a) or 250 μM (b).

The toxicity of a series of the pyrimidine oxides **3** was also investigated using the porcine embryo kidney (PEK) cell line. It was shown that **3a**, displaying no antiproliferative activity, also showed no acute (24 h) or chronic (7 d) toxicity in the concentrations up to of 50 μM. Compound **3n**, on contrary, was found to be quite toxic, possessing $CC_{50} < 6.25$ μM. In the terms of selectivity it was shown **3i** to be more promising, as it revealed no acute (24 h) toxicity up to of 50 μM, nevertheless it possessed $CC_{50} = 9.2 \pm 3.1$ μM.

For compounds **3a**, which have shown no citotoxic activity, and **3n**, found to be the most active species, the cell uptake behavior on MCF7 and HCT116 cell lines was investigated and visualized. After incubation with 25 μM or 250 μM of a pyrimidine *N*-oxide for 1 hour the cells were excited and the pictures were obtained (Figure 6). Both compounds **3a** and **3n** were shown to be readily accumulated in cells. No difference was observed for active and inactive

compounds that testifies that the lack of cytotoxicity of **3a** is not connected with its ability to enter the cell. Two investigated cancer cell lines showed no notable difference in the cell uptake either. The growth of the **3a** or **3n** concentration in the medium led to the fluorescence enhancement, probably, due to further accumulation of the substances inside the sells. Intensive fluorescence of the cells contour may point to the predominant accumulation of the pyrimidine oxides **3a,n** in cell membrane due to their hydrophobic properties.

Thus, depending on the substituents in the position *2* of the pyrimidine moiety the compounds **3** may possess significantly varying biological activity. Pyrimidine *N*-oxide **3a** possesses excellent biocompatibility and is capable to enter cells, that makes it a promising structure for development of bioimaging fluorescent probes, while antiproliferative activity found for **3b,i,n** and selectivity, shown by **3i**, allow to expect that further structural modification will lead to the structures, combining fluorescent properties, anticancer activity and high therapeutic index.

4. Conclusions

In summary, we have investigated a series of 2-methyl substituted pyrimidine *N*-oxides, bearing the substituents of various electronic nature, in the reaction with aromatic aldehydes. Basing on the studied reaction, the preparative approach to novel π-conjugated systems, containing pyrimidine *N*-oxide core, was elaborated and a series of previously unknown push-pull molecules were synthesized. Their photophysical properties were examined and it was found that all compounds possess the emission maxima more than 500 nm (up to 575 nm for compound **3o**, containing a perylenyl moiety). This redshift together with the either biocompatibility or antitumor activity, found for some of the obtained conjugated molecules, makes them promising compounds for various bioapplications.

Acknowledgements

We thank the Russian Foundation for Basic Research (project 18-03-00651-a) for financial support of this work. This study was fulfilled using a STOE STADI VARI PILATUS-100K

diffractometer and NMR spectrometer Agilent 400-MR purchased by MSU Development Program. The research is supported in part by the National Science Foundation, CHE-1665342. MTT-test is made with the financial support of the Russian Science Foundation (grant No. 14-03-00483).

References

1. For reviews see: (a) G. W. Rewcastle, in *Comprehensive Heterocyclic Chemistry III*, ed. A. R. Katritzky, C. A. Ramsden, E. F. V. Scriven and R. J. K. Taylor, Elsevier Ltd., Oxford, 2008, **8**, 120; (b) M. Baumann and I. R. Baxendale, *Beilstein J. Org. Chem.*, 2013, **9**, 2265; (c) S. Prachayasittikul, R. Pingaew, A. Worachartcheewan, N. Sinthupoom, V. Prachayasittikul, S. Ruchirawat and V. Prachayasittikul, *Mini-Rev. Med. Chem.*, 2017, **17**, 869.

2. For recent examples see: (a) M. Beesu, A. C. D. Salyer, M. J. H. Brush, K. L. Trautman, J. K. Hill and S. A. David, *J. Med. Chem.*, 2017, **60**, 2084; (b) X. Liang, F. Lv, B. Wang, K. Yu, H. Wu, Z. Qi, Z. Jiang, C. Chen, A. Wang, W. Miao, W. Wang, Z. Hu, J. Liu, X. Liu, Z. Zhao, L. Wang, S. Zhang, Z. Ye, C. Wang, T. Ren, Y. Wang, Q. Liu and J. Liu, *J. Med. Chem.*, 2017, **60**, 1793, (c) L. R. Odell, M. K. Abdel-Hamid, T. A. Hill, N. Chau, K. A. Young, F. M. Deane, J. A. Sakoff, S. Andersson, J. A. Daniel, P. J. Robinson and A. McCluskey, *J. Med. Chem.*, 2017, **60**, 349; (d) J. S. Debenham, C. Madsen-Duggan, M. J. Clements, T. F. Walsh, J. T. Kuethe, M. Reibarkh, S. P. Salowe, L. M. Sonatore, R. Hajdu, J. A. Milligan, D. M. Visco, D. Zhou, R. B. Lingham, D. Stickens, J. A. DeMartino, X. Tong, M. Wolff, J. Pang, R. R. Miller, E. C. Sherer and J. J. Hale, *J. Med. Chem.*, 2016, **59**, 11039; (e) J. H. Ryu, J. A. Lee, S. Kim, Y. A. Shin, J. Yang, H. Y. Han, H. J. Son, Y. H. Kim, J. H. Sa, J.-S. Kim, J. Lee, J. Lee and H.-g. Park, *J. Med. Chem.*, 2016, **59**, 10176.

3. (a) S. Achelle and N. Plé, *Curr. Org. Synth.*, 2012, **9**, 163; (b) S. Achelle, J. Rodrıguez-Lopez and F. Robin-le Guen, *J. Org. Chem.*, 2014, **79**, 7564; (c) S.-i. Kato, Y. Yamada, H. Hiyoshi, K. Umezu and Y. Nakamura, *J. Org. Chem.*, 2015, **80**, 9076; (d) Z. Zhang, J. Xie, H. Wang, B. Shen, J. Zhang, J. Hao, J. Cao and Z. Wang, *Dyes and Pigments*, 2016, **125**, 299; (e) S.

602 Achelle, J. Rodríguez-López, C. Katan and F. Robin-le Guen, *J. Phys. Chem. C*, 2016, **120**,
603 26986; (f) M. Mao, X. Zhang, B. Zhu, J. Wang, G. Wu, Y. Yin and Q. Song, *Dyes and Pigments*,
604 2016, **124**, 72; (g) M. Klikar, P. Poul, A. Růžička, O. Pytela, A. Barsella, K. D. Dorkenoo, F.
605 Robin-le Guen, F. Bureš and S. Achelle, *J. Org. Chem.*, 2017, **82**, 9435.
606 4. Y. Suzuki, J.-i. Sawada, P. Hibner, H. Ishii, K. Matsuno, M. Sato, B. Witulski and A.
607 Asai, *Dyes and Pigments*, 2017, **145**, 233.
608 5. (a) A. K. Gupta and A. Charrette, *Skinmed*, 2015**, 13***,* 185; (b) M. Barbareschi, *G. Ital.*
609 *Dermatol. Venereol.*, 2018, **153**, 102.
610 6. A. M. Mfuh and O. V. Larionov, *Curr. Med. Chem.*, 2015, **22**, 2819.
611 7. (a) A. R. Katritzky and J. M. Lagowski, *Chemistry of the Heterocyclic N-Oxides*,
612 Academic Press, New York, N.Y., 1971; (b) A. Angelo and S. Pietra, *Heterocyclic N-Oxides*,
613 CRC Press, Boca Raton, Florida, Inc., 1991; (c) D.W. Boykin, P. Balakrishnan and A. L.
614 Baumstark, *J. Heterocyclic Chem.*, 1985, **22**, 981.
615 8. (a) K. N. Sedenkova, E. B. Averina, Y. K. Grishin, A. G. Kutateladze, V. B. Rybakov, T.
616 S. Kuznetsova and N. S. Zefirov, *J. Org. Chem.*, 2012, **77**, 9893; (b) K. N. Sedenkova, E. B.
617 Averina, Y. K. Grishin, T. S. Kuznetsova and N. S. Zefirov, *Tetrahedron Lett.*, 2014, **55**, 483; (c)
618 K. N. Sedenkova, E. B. Averina, Y. K. Grishin, A. B. Bacunov, S. I. Troyanov, I. V. Morozov, E.
619 B. Deeva, A. V. Merkulova, T. S. Kuznetsova and N. S. Zefirov, *Tetrahedron Lett.*, 2015, **56**,
620 4927; (d) K. N. Sedenkova, E. V. Dueva, E. B. Averina, Y. K. Grishin, D. I. Osolodkin, L. I.
621 Kozlovskaya, V. A. Palyulin, E. N. Savelyev, B. S. Orlinson, I. A. Novakov, G. M. Butov, T. S.
622 Kuznetsova, G. G. Karganova and N. S. Zefirov, *Org. Biomol. Chem.*, 2015, **13**, 3406; (e) K. N.
623 Sedenkova, E. B. Averina, Yu. K. Grishin, T. S. Kuznetsova and N. S. Zefirov, *Russ. Chem. Bull.*,
624 2016, **65**, 1750; (f) K. N. Sedenkova, E. B. Averina, Y. K. Grishin, J. V. Kolodyazhnaya, V. B.
625 Rybakov, D. A. Vasilenko, D. V. Steglenko, V. I. Minkin, T. S. Kuznetsova and N. S. Zefirov,
626 *Tetrahedron Lett.*, 2017, **58**, 2955; (g) K. N. Sedenkova, E. B. Averina, Yu. K. Grishin, J. V.
627 Kolodjashnaja, V. B. Rybakov, T. S. Kuznetsova, A. Hughes, G. d. P. Gomes, I. Alabugin and N.

S. Zefirov, *Org. Biomol. Chem.*, 2017, **15**, 9433; (h) K. N. Sedenkova, E. B. Averina, A. A. Nazarova, Yu. K. Grishin, D. S. Karlov, V. L. Zamoyski, V. V. Grigoriev, T. S. Kuznetsova and V. A. Palyulin, *Mendeleev Commun.*, 2018, **28**, 423; (i) K. N. Sedenkova, A. A. Nazarova, E. V. Khvatov, E. V. Dueva, A. A. Orlov, D. I. Osolodkin, Y. K. Grishin, T. S. Kuznetsova, V. A. Palyulin and E. B. Averina, *Mendeleev Commun.*, 2018, **28**, 592.

9. A. M. Brouwer, *Pure Appl. Chem.*, 2011, **83**, 2213.

10. (a) G.M. Sheldrick, *Acta Cryst.*, 2008, **A64**, 112; (b) G.M. Sheldrick, *Acta Cryst.*, 2015, **C71**, 3; (c) L.J. Farrugia, *J. Appl. Cryst.*, 1997, **30**, 568; (d) A.L. Spek, *J. Appl. Cryst.*, 2003, **36**, 7.

11. M. Niks and M. Otto, *J. Immunol. Meth*., 1990, **130**, 149.

12. (a) A. A. Orlov, A. A.Chistov, L. I. Kozlovskaya, A. V. Ustinov, V. A. Korshun, G. G. Karganova and D. I. Osolodkin, *Med. Chem. Commun.*, 2016, **7**, 495; (b) M. A. Hamilton, R. C. Russo and R. V. Thurston, *Environ. Sci. Technol.*, 1977, **11**, 714.

13. For recent examples see: (a) G. M. Nepomuceno, K. M. Chan, V. Huynh, K. S. Martin, J. T. Moore, T. E. O'Brien, L. A. E. Pollo, F. J. Sarabia, C. Tadeus and Z. Yao, *ACS Med. Chem. Lett.*, 2015, **6**, 308; (b) B. S. Reddy, M. Rafeek, C. V. R. Reddy and P. K. Dubey, *Heterocycl. Lett.*, 2015, **5**, 105; (c) E. N. Agbo, T. J. Makhafola, Y. S. Choong, M. J. Mphahlele and P. Ramasami, *Molecules*, 2016, **21**, 28; (d) T. M. Aliyeu, D. V. Berdnikova, O. A. Fedorova, E. N. Gulakova, C. Stremmel and H. Ihmels, *J. Org. Chem.*, 2016, **81**, 9075.

14. (a) H. Yamanaka, S. Ogawa and S. Konno, *Chem. Pharm. Bull.*, 1980, **28**, 1526; (b) A. Kövendi and M. Kircz, *Chem. Ber.*, 1965, **98**, 1049; (c) F. Heaney and E. Lawless, *J. Heterocyclic Chem.,* 2007, **44**, 569; (d) R. Zimmer, T. Lechel, G. Rancan, M. K. Bera and H.-U. Reissig, *SYNLETT*, 2010, 1793; (e) E. Lewandowska and D. C. Chatfield, *Eur. J. Org. Chem.*, 2005, 3297.

15. For selected examples see: (a) G. E. Magoulas, S. E. Bariamis, C. M. Athanassopoulos and D. Papaioannou, *Tetrahedron Lett.*, 2010, **51**, 1989; (b) J.-C. Muller and H. Ramuz, *Helv. Chim. Act.*, 1982**, 65**, 1445; (c) H. Yamanaka, S. Ogawa and S. Konno, *Chem. Pharm. Bull.*, 1981, **29**, 98.

16. (a) H. Yamanaka, T. Sakamoto and S. Niitsuma, *Heterocycles*, 1990, **31**, 923; (b) M. Maltese, *J. Org. Chem.*, 1995**, 60,** 2436.

17. (a) J. Mei, N. L. C. Leung, R. T. K. Kwok, J. W. Y. Lam and B. Z. Tang, *Chem. Rev.*, 2015, **115**, 11718; (b) J. Chen, M. Liu, Q. Huang, L. Huang, H. Huang, F. Deng, Y. Wen, J. Tian, X. Zhang and Y. Wei, *Chem. Engineer. J.*, 2018, **337**, 82; (c) X. Zhang, K. Wang, M. Liu, X. Zhang, L. Tao, Y. Chen and Yen Wei, *Nanoscale*, 2015, **7**, 11486; (d) X. Zhang, X. Zhang, B. Yang, M. Liu, W. Liu, Y. Chena and Yen Wei, *Polym. Chem.*, 2014, **5**, 356; (e) X. Zhang, X. Zhang, B. Yang, M. Liu, W. Liu, Y. Chena and Yen Wei, *Polym. Chem.*, 2014, **5**, 399; (f) H. Huang, M. Liu, Q. Wan, R. Jiang, D. Xu, Q. Huang, Y. Wen, F. Deng, X. Zhang and Y. Wei, *Mater. Sci. Eng. C*, 2018, **91**, 201; (g) R. Jiang, M. Liu, C. Li, Q. Huang, H. Huang, Q. Wan, Y. Wen, Q.-y. Cao, X. Zhanga and Y. Wei, *Mater. Sci. Eng. C*, 2017, **80**, 708; (h) Z. Chen, J. Zhang, M. Song, J. Yin, G.-A. Yu and Sheng Hua Liu, *Chem. Commun.*, 2015, **51**, 326; (i) Z. Chen, G. Liu, S. Pu and S. H. Liu, *Dyes and Pigments*, 2017, **143**, 409.

18. (a) L. Yuan, W. Lin, K. Zheng, L. He and Weimin Huang, *Chem. Soc. Rev.,* 2013, **42**, 622; (b) R. Jiang, M. Liu, H. Huang, L. Mao, Q. Huang, Y. Wen, Q.-y. Cao, J. Tian, X. Zhang and Y. Wei, *Dyes and Pigments*, 2018, **151**, 123; (c) J. Tian, R. Jiang, P. Gao, D. Xu, L. Mao, G. Zeng, M. Liu, F. Deng, X. Zhang and Y. Wei, *Mater. Sci. Eng. C*, 2017, **79**, 563; (d) Y. Liu, L. Mao, X. Liu, M. Liu, D. Xu, R. Jiang, F. Deng, Y. Li, X. Zhang and Y. Wei, *Mater. Sci. Eng. C*, 2017, **79**, 590; (e) R. Jiang, H. Liu, M. Liu, J. Tian, Q. Huang, H. Huang, Y. Wen, Q.-y. Cao, X. Zhanga and Y. Wei, *Mater. Sci. Eng. C*, 2017, **81**, 416; (f) R. Jiang, M. Liu, T. Chen, H. Huang, Q. Huang, J. Tian, Y. Wen, Q.-y. Cao, X. Zhang and Y. Wei, *Dyes and Pigments*, 2018, **148**, 52.